Vibrational Relaxation of Cyanide on Copper Surfaces: Can Metal d-bands Influence Vibrational Energy Transfer?†

Christopher Matranga,‡ Brian L. Wehrenberg, and Philippe Guyot-Sionnest*

James Franck Institute, University of Chicago, 5640 S. Ellis, Chicago, Illinois 60637

Received: March 5, 2002; In Final Form: June 3, 2002

The lifetime for the CN^- stretching mode has been measured at a polycrystalline Cu and Cu(111) electrochemical interface with difference frequency generation. The lifetimes on both surfaces are ∼17 ps, show no definitive trend with electrochemical potential, and are similar to those reported for the CN^-/Au system. When all experimental lifetimes for CN^- on metals are considered, a trend is noted between vibrational lifetime and the onset of metal interband transitions.

Introduction

The study of adsorbate vibrations on surfaces plays a significant role in our understanding of surface−adsorbate interactions. The magnitude and direction of vibrational frequency shifts upon chemisorption and the dependence of these shifts on adsorption site yield information about the orbitals involved in bonding. Vibrational relaxation is also an important process to consider because the vibrational lifetime, its dependence on substrate composition, and the decay mechanism of the excited vibration are tied to the bonding interaction between the adsorbate and the surface. Vibrational energy relaxation can also influence the kinetics of surface processes such as sticking, diffusion, dissociation, and desorption. These processes can impact technologies ranging from chemical vapor deposition to catalysis.

Most studies of vibrational energy relaxation have been performed on the CO adsorbate.[1−14] Experimentally, relaxation of the CO stretching mode is a rapid process and lifetimes of ∼2 ps are found for CO on Cu(100) and Pt(111) in an ultrahigh vacuum environment.[6,7] In an electrochemical cell, lifetimes of roughly 2 ps are also found for CO on Pt(100) and Pt(111).[9,10] Semiempirical estimates and molecular orbital calculations for CO on Cu surfaces find a strong coupling for CO/Cu and the fast relaxation observed in the experiments is attributed to a charge-transfer mechanism.[1,3−5] All of these findings show that the vibrational relaxation of CO on metals is a rapid process (∼2 ps) and is relatively insensitive to the metal and its crystallographic orientation as well as to the surrounding environment.

Many current bonding and energy transfer models are based on these types of studies on the CO adsorbate.[1,3−5] To fully understand chemisorption, vibrational relaxation, and other properties which are influenced by these processes (e.g., reactivity) one must clarify how these properties change with different adsorbates. An ideal adsorbate to consider is CN^- because it is isoelectronic to CO. Because CN^- is ionic, one intuitively expects its interaction with the surface to differ from CO. One simple example of the different properties of these two adsorbates lies in how the CN^- stretching frequency increases by ∼80 cm^{-1} upon chemisorption to metals whereas the CO stretching frequency decreases by ∼70 cm^{-1}.[17] Recent calculations for the CO/Pt(111) and CN/Pt(111) systems attribute this to different bonding for the two adsorbates.[17]

Another interesting difference, for these two adsorbates, stems from lifetime measurements of the CN^- stretching mode in an electrochemical environment.[15,16] For CN^-, the lifetimes show a clear dependence on the metal, the potential and the electrolyte. Lifetimes are 3−6 ps on Pt(111) and 10−20 ps on Au. On Ag, solvent limited lifetimes are found which yield estimates in excess of 300 ps for vibrational relaxation to the surface. The magnitude of these lifetimes and the dependence on metal substrate are unlike the ∼2 ps for CO relaxation on metals.

Lifetime measurements for CN^- on other metals will help explain the different vibrational behaviors that CN^- and CO exhibit. It is also, in principle, easier to perform theoretical calculations on Cu than Ag, Au, or Pt and this motivates our current measurements for CN^-. We report here on the vibrational relaxation of CN^- on polycrystalline Cu and on Cu(111) in an electrochemical environment. Our measurements involve the detection of the CN^- adsorbate with sum frequency generation (SFG) and difference frequency generation (DFG).

Experimental Section

Measurements were made in a Teflon spectroelectrochemical cell which has been described previously.[15,16] All electrochemical potentials are reported with respect to a saturated calomel electrode (SCE).

Cu samples were electropolished with the following procedure:[18] (i) anodic etching for ∼40 s at 2 V in 85% orthophosphoric acid (degassed with argon) with a Pt foil cathode; (ii) rinsed with ultrapure H_2O and transferred in degassed H_2O to the electrochemical cell under potential control (−1.0 V/SCE). The surface orientation and cleanliness of Cu(111) (MaTeck, Germany) samples prepared with this procedure was checked with voltametry in acidic (pH ≈ 3.5) 0.1 M $NaClO_4$ and compared to the literature.[19] Spectroscopic studies on polycrystalline Cu and Cu(111) were conducted in neutral 0.1 M $NaClO_4$ and the cleanliness of these samples was checked by the sharp onset of H_2 production in the voltametry.

Cyanide adsorption was done by introducing a 25mM CN^- + 0.1 M $NaClO_4$ solution into the electrochemical cell at −1.2

† Part of the special issue "John C. Tully Festschrift".

* To whom correspondence should be addressed.

‡ Present address: U. S. Department of Energy, National Energy Technology Laboratory, P.O. Box 10940, Pittsburgh, Pennsylvania 15236-0940.

10.1021/jp020618q CCC: $22.00
Published on Web 07/03/2002

V/SCE. The sample was held at this potential in the cyanide containing solution for approximately 15 min before pressing the sample against the CaF_2 window for spectroscopic studies.

The laser system is based on an active-passive mode locked Nd:Yag laser which has been described previously.[20] The frequency doubled pulse train from this laser is used to pump a grating tuned optical parametric oscillator (OPO) producing tunable near-IR light between ~1.2−1.8 μm. The output of the OPO is mixed in a second parametric process with the single pulse 1064 nm output of the Nd:Yag in a $AgGaS_2$ crystal. This results in a tunable mid-IR pulse for spectroscopic studies. For this experiment, 7 ps pulses tunable near 2100 cm^{-1} with 40 μJ of energy are used. SFG and DFG spectra were taken with this mid-IR pulse and a visible 532 nm pulse obtained from the doubled output of the Nd:Yag laser.

SFG spectra from an adsorbate covered metal surface have a contribution from both adsorbate and metal. The intensity of the SFG spectra, I_{SFG}, can be modeled with the following equation[21,22]

$$I_{SFG} \propto \left|\frac{\langle i|\mu|f\rangle\left(\frac{d\sigma}{d\Omega}\right)_{AS}^{1/2}}{(\omega_{IR}-\omega_{res})+i\Gamma_{res}}\Delta n + Ae^{i\varphi}\right|^2 \qquad (1)$$

where $<i|\mu|f>$ is the dynamic dipole moment of an adsorbate vibration, $(d\sigma/d\Omega)_{AS}$ is the antistokes Raman cross section, Δn is the population difference between the ground and excited vibrational states, ω_{IR} is the energy of the IR beam used in the sum frequency process, ω_{res} is the resonance energy of an adsorbate vibration, and Γ_{res} is the line width. The first term in eq 1 is the resonant molecular contribution. The substrate contribution, $Ae^{i\varphi}$, is treated as a constant that has a phase and magnitude with respect to the molecular contribution.

For metals where the interband transition is near that of ω_{SFG} or ω_{VIS}, the nonresonant contribution to I_{SFG} is observed to be large. If the molecular contribution to the signal is out of phase from the nonresonant background, a dip in I_{SFG} will appear at resonance. This dip poses problems for systems where I_{SFG} is already near the threshold of detection.

Most SFG experiments use the doubled output (532 nm) of a Nd:Yag laser for ω_{VIS} so metals such as copper and gold become more difficult to work with because they have interband transitions near this frequency. This difficulty is reduced by using difference frequency generation (DFG).[21,22] The signal, I_{DFG}, for a DFG spectrum can be modeled with the following equation[21,22]

$$I_{DFG} \propto \left|\frac{\langle i|\mu|f\rangle\left(\frac{d\sigma}{d\Omega}\right)_{S}^{1/2}}{(\omega_{IR}-\omega_{res})-i\Gamma_{res}}\Delta n + Ae^{i\varphi}\right|^2 \qquad (2)$$

where $(d\sigma/d\Omega)_S$ is the Stokes Raman cross section and all other parameters are as defined in eq 1.

The significant difference between eq 1 and 2 is the sign in front of Γ_{res}. This sign difference causes a 180° phase change between the imaginary components of the molecular and substrate contributions between SFG and DFG. As a result, a line shape which appears as a dip in I_{SFG} will appear as a peak in I_{DFG}, thus making the vibrational spectra easier to detect.

For time-resolved studies, the mid-IR pulse is split into a pump and probe beam. To ensure optimal spatial and temporal overlap of all beams, a nonresonant SFG signal was first generated from a clean Au coated slide in the electrochemical cell. The SFG signal is optimized with the probe/visible and pump/visible, then all three pulses are aligned with four wave mixing ($\omega_3 = \omega_{probe} + \omega_{pump} + \omega_{vis}$) on the surface. This procedure creates an optimal alignment and the most efficient pumping of the CN^- stretching mode. After this alignment, it is straightforward to switch between either SFG or DFG studies by only changing the output alignment of the system. For the current study, only DFG is used for time-resolved measurements. The saturation of the DFG signal, $S(t)$, is analyzed as $1 - (S(t)/S_o)^{1/2}$ as a function of delay time between the pump beam and the DFG probe. This yields the temporal dependence of twice the excited-state population, $2n_1(t)$, in a two level system. Saturation levels, $n_1(t)$, between 5% and 15% are obtained.

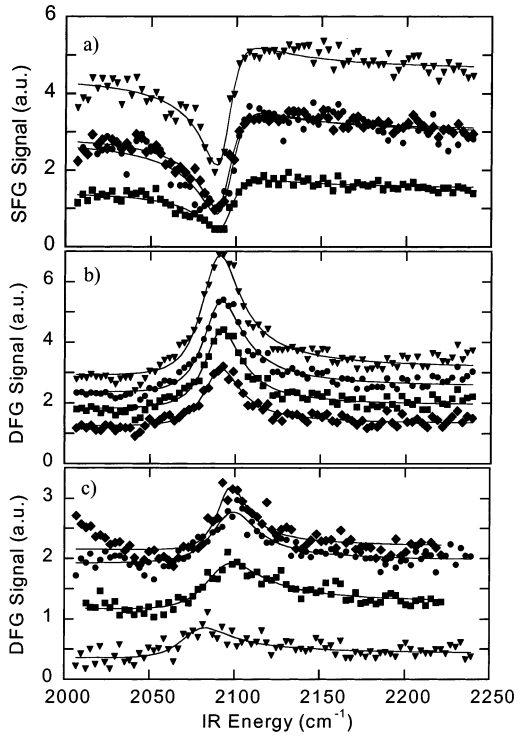

Figure 1. Vibrational spectra of CN^- on polycrystalline Cu and Cu(111). (a) SFG spectra of CN/Cu at −0.9 V/SCE (circles), −1.0 V/SCE (squares), −1.1 V/SCE (diamonds), and −1.2 V/SCE (triangles). Solid lines are fits to eq 1. (b) DFG spectra of CN^-/Cu at various potentials [same key as (a)]. Solid lines are fits to eq 2. (c) DFG spectra of CN^-/Cu(111) [same key as (a) and (b)]. DFG Spectra are fit to eq 2 (solid lines).

Results

Figure 1a shows SFG spectra of CN^- on polycrystalline copper. The DFG spectra for CN^-/Cu are shown in Figure 1b. As discussed above, the vibrational resonance, which is a dip in the SFG spectra, appears as a peak in the DFG signal. The SFG/DFG spectra of CN^-/Cu show a single resonance with no significant potential tuning. DFG spectra for the CN^-/Cu(111) are shown in Figure 1c. Again, a single resonant peak is seen with no real potential dependence. The peak for CN^-/Cu(111) is broader than for the polycrystalline system. The *y*-axis for each spectrum in Figure 1a−c has not been artificially offset. The magnitude changes are a result of potential dependent changes in the nonresonant background.

Representative saturation curves are shown in Figure 2a,b. The saturation data are described with a simple exponential decay. The lifetimes are ~17 ± 2 ps on polycrystalline Cu and ~18 ± 4 ps on Cu(111), and lack any definitive potential trend within the small potential range available for studies of CN^- on copper (−1.2 to - −0.9 V/SCE). At more positive potentials

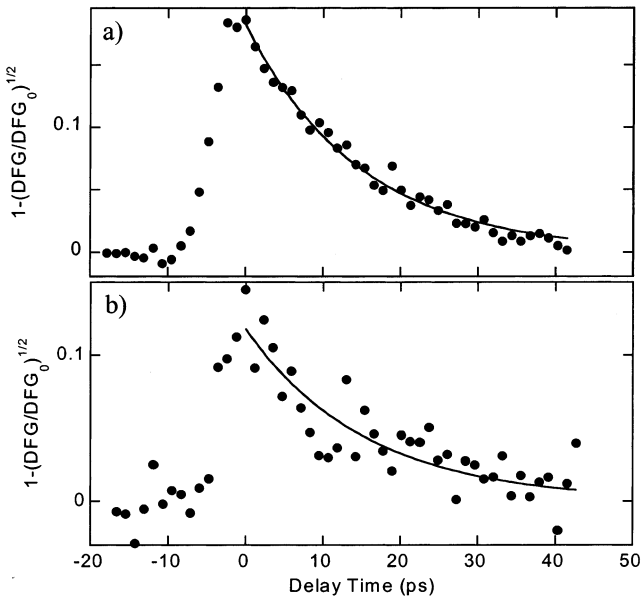

Figure 2. (a) Vibrational decay of CN^-/Cu at −1.2 V/SCE as probed by DFG spectroscopy. Solid dots are experimental data and the line is a single-exponential fit yielding $T_1 = 14.8$ ps. (b) Same as (a) but for CN^-/Cu(111) at −1.0 V/SCE ($T_1 = 15.6$ ps).

etching occurs and at more negative potentials hydrogen evolution occurs.

Discussion

Previously, the long lifetimes of CN^- on metals were interpreted in the context of an image-dipole relaxation.[15] In this model, the vibrational mode is treated as a radiating point dipole for which energy damping occurs thru excitation of electron−hole pairs in the metal. This type of coupling has been evaluated for the CO/Cu system yielding a lifetime of 8 ps for a 0.2 D dynamic dipole moment[2]. To estimate lifetimes for CN^-/Cu, we scale the result of the CO/Cu calculation with respect to the different dynamic dipole moment values estimated for CN^- on metals (0.13−0.16 D)[15] yielding a lifetime of 11−19 ps. This estimate is in good agreement with the lifetimes observed for CN^- on both polycrystalline Cu and Cu(111).

The image-dipole mechanism correctly accounts for the magnitude of CN^- lifetimes on metals, the trend with potential, and the lifetime variance with free-electron density parameters.[15] Also, the image-dipole mechanism can account for the extremely long lifetime ($T_1 > 300$ ps) for CN^-/Ag if one assumes that the CN^-/Ag bonding is predominately ionic.[15] This would produce an $[Ag^{\delta+}(CN)^{\delta-}]$ adlayer where the Ag atom still has some degree of bonding to the underlying substrate. This bonding should shift the image plane of the metal and weaken the coupling between the excited vibration and the electron density of the metal.[15]

If the bonding of CN^- to a metal surface could be reduced to the case of a simple metal anion ($[M^{\delta-} X^{\delta-}]$), the bond polarity should depend on the electronegativity value of the metal. The image plane shifting and thus vibrational lifetime from metal to metal should also display some trend with the electronegativity values for each metal. Considering all metals studied with the CN^- adsorbate, the Pauling electronegativity values are: 1.93 for Ag, 1.95 for Cu, 2.28 for Pt, and 2.54 for Au. On the basis of these values one would expect the lifetime trend: $\tau_{Ag} \approx \tau_{Cu} > \tau_{Pt} > \tau_{Au}$. Experimentally, one finds a different trend: $\tau_{Ag} \gg \tau_{Au} \approx \tau_{Cu} > \tau_{Pt}$. Clearly, the bonding of diatomics to metal surfaces is more complicated than the simple approximation of a metal anion. The lack of trend with electronegativity values may not be a failure of the image-dipole mechanism but instead related to interpreting bonding and image plane shifting in such a simple fashion. It is important, however, to consider other possibilities.

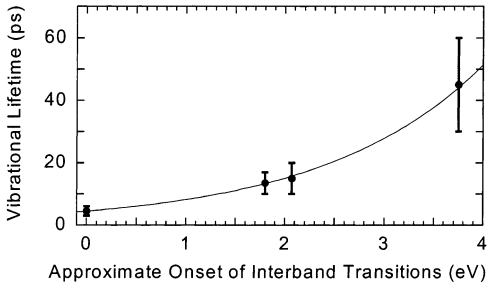

Figure 3. Relationship between vibrational lifetime of CN^- and the onset of interband transitions in the metal substrate. Data points for Pt(111), Au, and Ag are extracted from ref 15. Solid dots are the mean of the vibrational lifetime reported and error bars represent the range of lifetimes found in the study. For Ag, the experimental solvent limited lifetimes are used (30 ps in H_2O and 60 ps in D_2O) although relaxation to the metal was estimated in ref 15 to be 300 ps or greater. The solid line is meant only as a guide to the eye.

One interesting observation is that the vibrational lifetimes correlate with the onset of interband transitions for each of the metals (Figure 3): 0.0 eV for Pt, 1.8 eV for Cu, 2.1 for Au, and 3.75 eV for Ag.[23] Metal *d*-bands are known to play a role in the chemisorption of CO[24] and CN[17,25] on metals, but what role can they play in the vibrational relaxation? From an intuitive standpoint, the lifetime expressions for vibrational relaxation are derived from a golden rule formalism, where the density of states available for relaxation plays a role in the decay of excited states. One might expect to explain the lifetime trend by just considering the metal density of states at the Fermi level: Cu, Ag, and Au all have $\rho(\epsilon_f) \approx 0.3$ states/eV and Pt has $\rho(\epsilon_f) \approx 2.20$ states/eV.[23] However, it is important to keep in mind that in the charge transfer model it is the projected density of states of the metal on the adsorbate (e.g., mixing of states) not simply the metal density of states that dictate vibrational lifetimes. In the charge-transfer model, the following relaxation expression is found[1]

$$\frac{1}{\tau} = 2\pi\Omega(\rho(\epsilon_F)\delta\epsilon)^2 \qquad (3)$$

where Ω is the frequency of the vibrational mode, $\rho(\epsilon_F)$ is the projected density of states, and $\delta\epsilon$ is the fluctuation in the position of the resonance during the vibration.

Equation 3 predicts that a larger projected density of states near the Fermi level will lead to shorter charge-transfer lifetimes, therefore, in this model, the mixing of metal and adsorbate states is critical with respect to vibrational relaxation. The *sp*-band in all the metals studied is broad and of similar low density; therefore, it should not create major differences. On the other hand, if the *d*-bands play as significant a role in CN^- bonding on metals as suggested by previous calculations for CN/Pt-(111),[17] their mixing with adsorbate orbitals should contribute to the projected density of states. For CN, calculations have shown that the 5σ orbital pins near the metal Fermi level and mixes with metal states.[17] For the metal series Pt, Cu, Au, and Ag, the *d*-bands become situated further below the Fermi level of the metal and 5σ and *d*-band mixing should decrease as well. This would create a smaller projected density of states at the Fermi level and could account for the observed lifetime trends noted above for CN^-.

We note that this argument seems to conflict with the relaxation rates observed for CO/Pt and CO/Cu, both with $T_1 \approx 2$ ps.[6−11] Possibly, this is resolved by considering that CO bonding involves *d*-band mixing with both the $2\pi^*$ and 5σ orbitals[24] in contrast to CN where $2\pi^*$ is too far above the Fermi level to be involved. The similar lifetimes for CO on Cu and Pt could just be a coincidence where the projected density of states at the Fermi level are similar for both systems, thus yielding nearly identical vibrational lifetimes. A similar argument for the possibility of different slopes of the projected density of states was previously suggested and used to explain the discrepancy between the potential-dependent lifetimes observed for CO/Pt(111) and theoretical predictions for CO/Cu.[5,11]

The correlation between vibrational lifetime and *d*-bands is an interesting experimental observation that needs further clarification. Theoretical calculations such as the ones performed for CO/Cu[1,3−5] should help clarify how the metal *d*-bands affect vibrational relaxation for adsorbates on metals.

Summary

The vibrational lifetime of CN^- on polycrystalline Cu and Cu(111) was measured in an electrochemical environment with DFG spectroscopy. The vibrational lifetimes on both metals are ∼17 ps. The lifetimes are in agreement with estimates from the image-dipole relaxation mechanism.

However, when all metals studied with the CN^- adsorbate are considered, a trend is noted between the onset of metal interband transitions and the vibrational lifetime. This trend could be related to the role that the metal *d*-bands play on the projected density of states at the Fermi level. Further theoretical efforts for the CN^- adsorbate should help elucidate the role of metal *d*-bands on vibrational relaxation on metal surfaces.

References and Notes

(1) Persson, B. N. J.; Persson, M. *Solid State Commun.* **1980**, *36*, 175.
(2) Liebsch, A. *Phys. Rev. Lett*. **1985**, *54*, 67.
(3) Head-Gordon, M.; Tully, J. *J. Chem. Phys.* **1991**, *96*, 3939.
(4) Head-Gordon, M.; Tully, J. *Phys. Rev. B* **1992**, *46*, 1853.
(5) Head-Gordon, M.; Tully, J. *Chem. Phys.* **1993**, *175*, 37.
(6) Beckerle, J. D.; Cavanagh, R. R.; Casassa, M. P.; Heilweil, E. J.; Stephenson, J. C. *J. Chem. Phys.* **1991**, *96*, 5403.
(7) Morin, M.; Levinos, N. J.; Harris, A. L. *J. Chem. Phys.* **1991**, *96*, 3950.
(8) Beckerle, J. D.; Casassa, M. P.; Cavanagh, R. R.; Heilweil, E. J.; Stephenson, J. C. *Phys. Rev. Lett.* **1990**, *64*, 2090.
(9) Peremans, A.; Tadjeddine, A.; Guyot-Sionnest, P. *Chem. Phys. Lett.* **1995**, *247*, 243.
(10) Peremans, A.; Tajeddine, A.; Zheng, W. Q.; LeRille, A.; Guyot-Sionnest, P.; Thiry, P. A. *Surf. Sci.* **1996**, *368*, 384.
(11) Schmidt, M. E.; Guyot-Sionnest, P. *J. Chem. Phys.* **1995**, *104*, 2438.
(12) Bonn, M.; Hess, C.; Funk, S.; Miners, J.; Persson, B.; Wolf, M.; Ertl, G. *Phys. Rev. Lett.* **2000**, *84*, 4653.
(13) Hess, C.; Wolf, M.; Bonn, M. *Phys. Rev. Lett.* **2000**, *85*, 4341.
(14) Bonn, M.; Hess, C.; Wolf, M. *J. Chem Phys.* **2001**, *115*, 7725.
(15) Matranga, C.; Guyot-Sionnest, P. *J. Chem. Phys.* **2000**, *112*, 7615.
(16) Matranga, C.; Guyot-Sionnest, P. *Chem. Phys. Lett.* **2000**, *340*, 39.
(17) Daum, W.; Dederichs, F.; Muller, J. E. *Phys. Rev. Lett.* **1998**, *80*, 766.
(18) Akeman, W.; Friedrich, K. A.; Linke, U.; Stimming, U. *Surf. Sci.* **1998**, *402−404*, 571.
(19) Wong, E. K. L.; Friedrich, K. A.; Richmond, G. L. *Chem. Phys. Lett.* **1992**, *195*, 628.
(20) Guyot-Sionnest, P. *J. Electron Spectrosc. Relat. Phenom*. **1993**, *64/65*, 1.
(21) Tadjeddine, A.; Lerille, A.; Pluchery, O.; Vidal, F.; Zheng, W. Q.; Peremans, A. *Phys. Stat. Sol.* **1999**, *175*, 89.
(22) LeRille, A.; Tadjeddine, A. *J. Electroanal. Chem.* **1999**, *467*, 238.
(23) Papaconstantopoulos, D. A. *Handbook of Band Structure of Elemental Solids*; Plenum: New York, 1986.
(24) Hammer, B.; Morikawa, Y.; Norskov, J. K. *Phys. Rev. Lett.* **1996,** *76*, 2141
(25) Ample, F.; Curulla, D.; Fuster, F.; Clotet, A.; Ricart, J. *Surf. Sci.* **2002**, *497*, 139.